

Organic geochemical investigations of the Dali Lake sediments in northern China: Implications for environment and climate changes of the last deglaciation in the East Asian summer monsoon margin



Jiawei Fan^{a,*}, Jule Xiao^{a,b,*}, Ruilin Wen^a, Shengrui Zhang^a, Xu Wang^a, Linlin Cui^a, Hideki Yamagata^c

^a Key Laboratory of Cenozoic Geology and Environment, Institute of Geology and Geophysics, Chinese Academy of Sciences, Beijing 100029, China

^b College of Earth Sciences, University of Chinese Academy of Sciences, Beijing 100049, China

^c Paleo Labo Co., Ltd., Saitama 335-0016, Japan

ARTICLE INFO

Keywords:

Dali Lake
Sedimentary organic matter
Environment
Climate
East Asian summer monsoon
Last deglaciation

ABSTRACT

Millennial-scale environment and climate changes in the East Asian summer monsoon margin during the last deglaciation are reconstructed by systematic studies on the characteristic of sedimentary organic matter from Dali Lake in northern China. Concurrent increases in the TOC and TN concentrations indicate increases in terrestrial organic matter and nutrient inputs to the lake and a development of terrestrial vegetation and phytoplankton productivity related to increases in regional temperature and precipitation. C/N ratios reflect changes in the proportions of terrestrial and aquatic organic matter. Decreases in both $\delta^{13}\text{C}_{\text{org}}$ and $\delta^{15}\text{N}$ values indicate increases in the isotopically lighter, terrestrial carbon and nitrogen inputs to the lake, due to increases in surface runoffs; while a sharp decrease in the $\delta^{15}\text{N}$ value implies a significant weakening in the biological activities of nitrifying and ammonifying bacteria, due to abrupt decrease in the water temperature. The geochemical data indicate that regional temperature and precipitation exhibited increasing trends from 15,000 to 12,350 cal yr BP; temperature decreased abruptly at 12,350 cal yr BP and then maintained a low level from 12,350 to 11,400 cal yr BP, precipitation decreased to a relatively low level from 12,350 to 11,400 cal yr BP; and both temperature and precipitation returned to increase after 11,400 cal yr BP. The climate change in the Dali Lake region during the last deglaciation corresponds, within age uncertainties, to the Bølling-Allerød (BA) warm phase and Younger Dryas (YD) cold reversal occurring over northern high latitudes. However, the gradual and mild increasing trends of regional temperature and precipitation during the BA warm period contrasts with the general cooling trend in northern high latitude temperature, implying a dominant influence from increases in the Northern Hemisphere summer insolation; while the slight decreases in regional precipitation relative to the rapid and significant decreases in northern high latitude temperature during the YD cold period may have resulted from local moisture recycling or from an insensitive response of hydrology and ecology to the regional precipitation change.

1. Introduction

The last deglaciation is of special interest because this period represents the youngest transition from glacial to interglacial stages and it encompasses several distinct stages of significant climate changes such as the last glacial maximum (LGM), Heinrich stadial 1 (H1), Bølling-Allerød (BA) warm phase and Younger Dryas (YD) cold reversal over northern high latitudes (Heinrich, 1988; Dansgaard et al., 1993; Bond et al., 1997). Greenland ice cores have provided the high-resolution records of these marked climate fluctuations during the last

deglaciation (Grootes et al., 1993; Stuiver and Grootes, 2000; North Greenland Ice Core Project members, 2004; Rasmussen et al., 2006), and these climate fluctuations are suggested to have global impacts based on the evidence from both geological records from north-west Europe (Brooks and Birks, 2001), central North America (Yu and Eicher, 1998), Orca Basin in the northern Gulf of Mexico (Flower et al., 2004) and the Asian monsoon region (Wang et al., 2001; Yuan et al., 2004; Dykoski et al., 2005; An et al., 2012; Park et al., 2014; Russell et al., 2014; Chen et al., 2015) and from numerical models (COHMAP Members, 1988; Liu et al., 2009; Sun et al., 2012). In the

* Corresponding authors at: Key Laboratory of Cenozoic Geology and Environment, Institute of Geology and Geophysics, Chinese Academy of Sciences, Beijing 100029, China (J. Xiao).
E-mail addresses: jwfan@mail.iggcas.ac.cn (J. Fan), jlxiao@mail.iggcas.ac.cn (J. Xiao).

Asian monsoonal region, however, geological records exhibit prominent differences in the nature of these climate fluctuations (Yancheva et al., 2007; Liu et al., 2008; Hong et al., 2010; Stebich et al., 2011; Huang et al., 2012; Qiang et al., 2013; Zhou et al., 2016). For example, the palynological record of a sediment core from Qinghai Crater Lake in Yunnan Province in southwestern China implied a dry climate during the BA warm period and a wet climate during the YD cold period (Yang et al., 2016), while the total organic carbon (TOC) and CaCO_3 records from Qinghai Lake on the northeastern Tibetan Plateau (Shen et al., 2005; An et al., 2012) and the magnetic records from Gonghai Lake (Chen et al., 2013) in northern China suggested a wet climate during the BA warm period and a dry climate during the YD cold period. In addition, the oxygen isotopic record of stalagmite from Palawan indicated more gradual changes of the YD cold reversal in the tropical Pacific than in the northern high latitudes (Partin et al., 2015), while the pollen record from Suigetsu Lake in Japan suggested rapid changes of the YD cold reversal (Nakagawa et al., 2003). Therefore more independent proxy records from the Asian monsoon region are needed to provide additional insight into the characteristic of regional climate change during the last deglaciation and its possible driving mechanisms.

Several lakes are located in the East Asian summer monsoon (EASM) margin and are considered as ideal natural archives of past changes in the EASM precipitation (Xiao et al., 2004, 2008; Wen et al., 2010; Zhai et al., 2011; Zhang et al., 2012; Chen et al., 2015; Fan et al., 2016, 2017). The organic matter accumulated in lake sediments can be used to reflect changes in terrestrial vegetation development in the lake catchment, aquatic plant productivity within the lake, and hydrological conditions in the lake basin; thus constitutes a source of information about variations in the regional environment and climate during the geological past (Meyers and Teranes, 2001; Lamb et al., 2004; Herzschuh et al., 2005; Shen et al., 2005; Parplies et al., 2008; Zhu et al., 2008; Selvaraj et al., 2012).

Dali Lake is the second largest lake in Inner Mongolia in the EASM margin (Fig. 1). The lake water is alkaline (Fan et al., 2016) and consists mainly of planktonic algae with scarce emergent and submerged macrophytes (Li, 1993; Wang and Dou, 1998). In the lake catchment C_3 plants dominate the terrestrial vegetation (Wang et al.,

2003). These data imply that carbon and nitrogen signatures of sedimentary organic matter from Dali Lake would provide clear insights into the past environment and climate changes in the region. In the present study, we present high-resolution (~ 50 yr) records of TOC and TN concentrations, C/N ratios, $\delta^{13}\text{C}_{\text{org}}$ and $\delta^{15}\text{N}$ values of organic matter in a sediment core from Dali Lake. The main aim of the study is to use the dataset to reconstruct the environment and climate changes in the EASM margin during the last deglaciation and improve our understanding of the underlying driving mechanisms.

2. Regional setting

Dali Lake ($43^{\circ}13'–43^{\circ}23'$ N, $116^{\circ}29'–116^{\circ}45'$ E) is located in the northern margin of the E–W-extending Hulandaga Desert Land, 70 km west of Hexigten Banner, Inner Mongolia (Fig. 1), in an inland fault-depression basin that was formed in the Pliocene to Pleistocene (Li, 1993). The lake has an area of 238 km^2 , a maximum water depth of 11 m, an elevation of 1226 m above sea level (Fig. 1), and is hydrologically closed. Hills surround the lake to the north and west, and lacustrine plains are present along the eastern shore. Two permanent rivers, the Gongger and Salin Rivers, enter the lake from the northeast and two intermittent streams, the Holai and Liangzi Rivers, enter from the southwest (Fig. 1); however, there are no outflowing rivers. The Gongger River, the major inflow, rises in the southern terminal part of the Great Hinggan Mountains, where the elevation reaches 2029 m, and has a drainage area of 783 km^2 and a total channel length of 120 km (Li, 1993). Hydrological observations indicate that the discharge of the Gongger River is as large during spring floods in April as during summer floods in July, because of significant melt water runoff from the snow/ice packs covering the mountains (Li, 1993).

Dali Lake sits at the transition from semi-humid to semi-arid areas of the middle temperate zone. The climate of the region is controlled by the East Asian monsoon (An, 2000; Xiao et al., 2004). In region, mean annual temperature is 3.2°C with a July average of 20.4°C and a January average of -16.6°C (Fig. 2). Mean annual precipitation is 383 mm, and $\sim 70\%$ of the annual precipitation falls from June to August (Fig. 2). Mean annual evaporation reaches 1632 mm, which is more than 4 times the annual precipitation (Fig. 2). Dali Lake has a pH of 9.5, a salinity of 7.4 g/L and an alkalinity of 4.9 CaCO_3 g/L (Fan et al., 2016).

The modern natural vegetation of the Dali Lake basin is categorized as middle temperate steppe and is dominated by grasses (Compilatory Commission of Vegetation of China, 1980; Li, 1993). In the Hulandaga Desert Land, low-growing xerophilous plants including *Polygonum divaricatum*, *Agriophyllum squarrosum* and *Artemisia desteriorum* are present, together with the shrubs *Salix gordeivii*, *Ulmus pumila* and *Caragana sinica*. Herbs including *Stipa grandis*, *Leymus chinensis* and *Cleistogenes squarrosa* are developed in the northern and western hilly lands and on the eastern lacustrine plains. Forests consisting of *Larix gmelinii*, *Pinus tabuliformis*, *Betula platyphylla*, *Populus davidiana* and *Quercus mongolica* are distributed on the western slopes of the Great Hinggan Mountains, where the Gongger River rises, together with shrubs and herbs growing beneath the canopy.

Dali Lake has a secchi depth of ca. 1 m in the nearshore zone and 1.5 m in the offshore zone. Aquatic plants living in the lake consist mainly of planktonic algae with scarce vascular plants (Li, 1993; Wang and Dou, 1998). Planktonic algae include *Microcystis salina*, *Lyngbya contorta* and *Anabaenopsis muelleri* of the Cyanophyta, and *Surirella peisohispant*, *Amphiprorra paludo* and *Cyclotella meneghiniana* of the Bacillariophyta. Potamogetonaceae, including *Potamogeton crispus* and *Potamogeton pectinatus*, are the dominant aquatic vascular plants; they are generally confined to the areas of the river mouth where the water depth is less than 1.5 m.

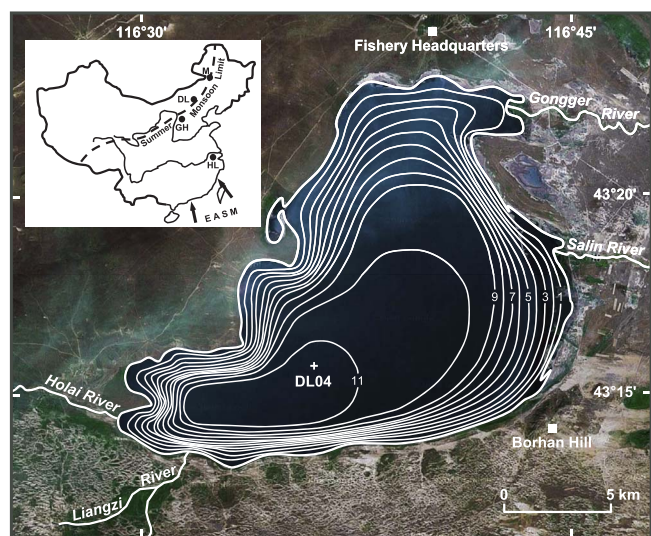


Fig. 1. Map of Dali Lake (from <http://maps.google.com>) showing the location of the DL04 sediment core (cross). The bathymetric survey of the lake was conducted in June 2002 using a FE-606 Furuno Echo Sounder (contours in m). The inset map shows the core locations of Dali Lake (DL) ($43^{\circ}15'$ N, $116^{\circ}36'$ E), Moon Lake (M) ($47^{\circ}30'$ N, $120^{\circ}52'$ E), Gonghai Lake (GH) ($38^{\circ}54'$ N, $112^{\circ}14'$ E) and Hulu Cave (HL) ($32^{\circ}30'$ N, $119^{\circ}10'$ E) in China (solid circles) and the modern northern limit of the East Asian summer monsoon defined by the 400-mm isohyet of mean annual precipitation (Xiao et al., 2004; An et al., 2012).

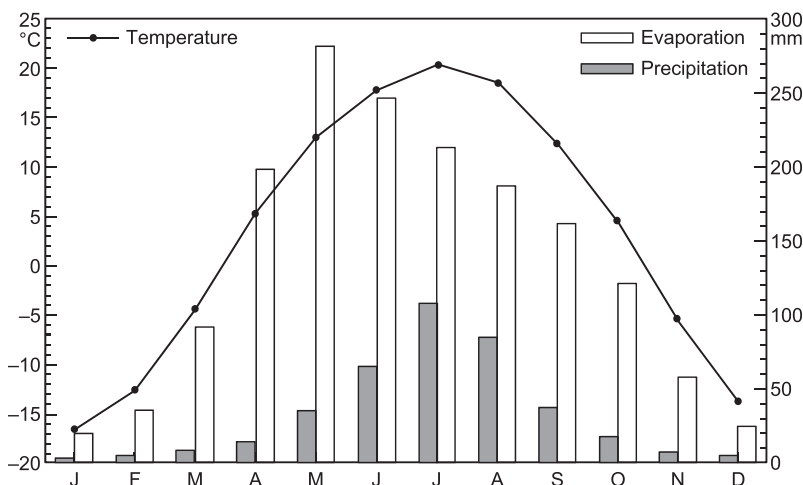


Fig. 2. Mean monthly temperature, mean monthly precipitation and mean monthly evaporation in the Dali Lake region. Data are the average of observations from 1981 to 2010 at Hexigten Banner Meteorological Station, 70 km east of Dali Lake (unpublished data courtesy of Inner Mongolia Meteorological Bureau).

3. Materials and methods

3.1. Sediment sampling and lithology

Sediment coring was conducted at a water depth of 10.8 m in the depocenter of Dali Lake in February 2004, when the lake surface was frozen (Fig. 1), using a TOHO drilling system (Model D1-B) (Toho Chikakoki Co., Ltd., Japan). Incremental sediment cores were extracted to a total depth of 11.83 m beneath the lake floor and were designated DL04 (43°15.68' N, 116°36.26' E) (Fig. 1). The cores were collected in polyethylene tubes using a piston corer of the drilling system, and sediment recovery was close to 100%.

The sedimentary organic carbon and nitrogen data from the upper 8.5 m of the DL04 core have been published in Fan et al. (2017) and the 11.25–11.83 m is lack of organic matter (TOC concentrations are less than 0.5%). In order to link with the previous work in Fan et al. (2017), the 7.7–11.25 m is used for the present study (Fig. 3). The sediments consist of blackish-grey to greenish-grey, massive silt, and can be divided into four main sedimentary units (Fig. 3), as follows: 1125–985 cm blackish-grey massive silt with greenish-grey bands at depths of 1125–1113 cm; 985–875 cm greyish-black massive silt; 875–789 cm blackish-grey massive silt; 789–770 cm greenish-grey massive silt with occasional blackish-grey bands. There is no indication of any sedimentary hiatuses based on lithology.

3.2. Chronology

Eight bulk samples from the 7.7 to 11.5 m of the DL04 core were radiocarbon dated using an Accelerator Mass Spectrometry (AMS) system (Compact-AMS, NEC Pelletron) at the Paleo Labo Co., Ltd. (Japan) (Table 1). Organic matter (~2 mg C) was extracted from each sample and dated following the method described by Nakamura et al. (2000). The ^{14}C dates of all the samples from the 7.7 to 11.5 m of the DL04 core were determined using a half-life of 5568 yr (Godwin, 1962).

The original radiocarbon dates are cited from Liu et al. (2016) in this study. The carbon reservoir effects are corrected using the method described in Fan et al. (2017). The reservoir-corrected ages are then converted to calibrated ages using the OxCal4.2 radiocarbon age calibration program (Bronk Ramsey and Lee, 2013) with IntCal13 calibration data (Reimer et al., 2013). The age–depth model is created by linear interpolation between radiocarbon-dated horizons using the mean values of 2σ ranges of calibrated ages. In general, the 7.7–11.25 m of the DL04 core covers the age from 15,000 to 10,000 cal yr BP (Fig. 3; Table 2). The sedimentation rates of ca. 50–120 cm/kyr and sampling intervals of 2–5 cm provide potential temporal resolu-

tions of ca. 30–80 yr for the sedimentary organic carbon and nitrogen data from the 7.7 to 11.25 m of the core.

3.3. Analyses of TOC and TN concentrations

The data of TOC and TN concentrations from the 7.7 to 8.5 m of the DL04 core are cited from Fan et al. (2017). The 8.5–11.25 m of the core are sampled at 2–5-cm intervals for measurements of TOC and TN concentrations ($n = 67$). TOC concentrations are determined with an Elementar High TOC II analyzer. Samples are ground into powder finer than $85\ \mu\text{m}$ and dried at $110\ ^\circ\text{C}$ for 24 h. Each sample is separately weighed to ~300 mg and ~30 mg for analyses of total carbon (TC) and total inorganic carbon (TIC), respectively. In order to completely convert carbon to CO_2 , samples for TC analysis are fully combusted at $1150\ ^\circ\text{C}$; whereas samples for TIC analysis are reacted in excess 9% HCl. A reference soil sample, GBW07402, is separated into four weighed portions with two portions for TC and another two for TIC and routinely analyzed in parallel with the samples each day. All of the TC and TIC values are normalized to GBW07402, the certified TC and TIC values of which are 0.75% and 0.26%, respectively. The High TOC II yields the TC and TIC concentrations of a sample with a relative error of $\leq 1\%$. The TOC value is the difference between the TC and TIC concentrations.

TN concentrations are determined with a Yanaco CHN Corder MT-5 analyzer. Samples are ground to a powder finer than $61\ \mu\text{m}$ and dried at $40\ ^\circ\text{C}$ for 24 h. Each sample of 50 mg of dried sediment is fully combusted at $450\ ^\circ\text{C}$ for 5 min to completely convert nitrogen to NO_x , and the resulting NO_x is then reduced to N_2 by copper. A reference Antipyrine sample (SMA-SP-9), is separated into three weighed portions and routinely analyzed after every thirty sample measurements. All of the TN values are normalized to SMA-SP-9, the certified TN value of which is 14.88%. The relative analytical error of the TN concentration of a sample is less than 0.3%.

TOC/TN (C/N) is expressed as an atomic ratio calculated using a ratio of 1.17 between the atomic and mass ratios (Meyers, 1994; Lamb et al., 2006).

3.4. Analyses of organic carbon and nitrogen isotopic composition

The data of $\delta^{13}\text{C}_{\text{org}}$ and $\delta^{15}\text{N}$ values from the 7.7 to 8.5 m of the DL04 core are cited from Fan et al. (2017). The 8.5–11.25 m of the core is sampled at 2–5-cm intervals for measurements of organic carbon and nitrogen isotopic composition ($n = 67$). Carbon and nitrogen isotopic composition are determined with a Delta V Plus mass spectrometer equipped with a Thermo Flash EA 1112 element analyzer and a ConFlo

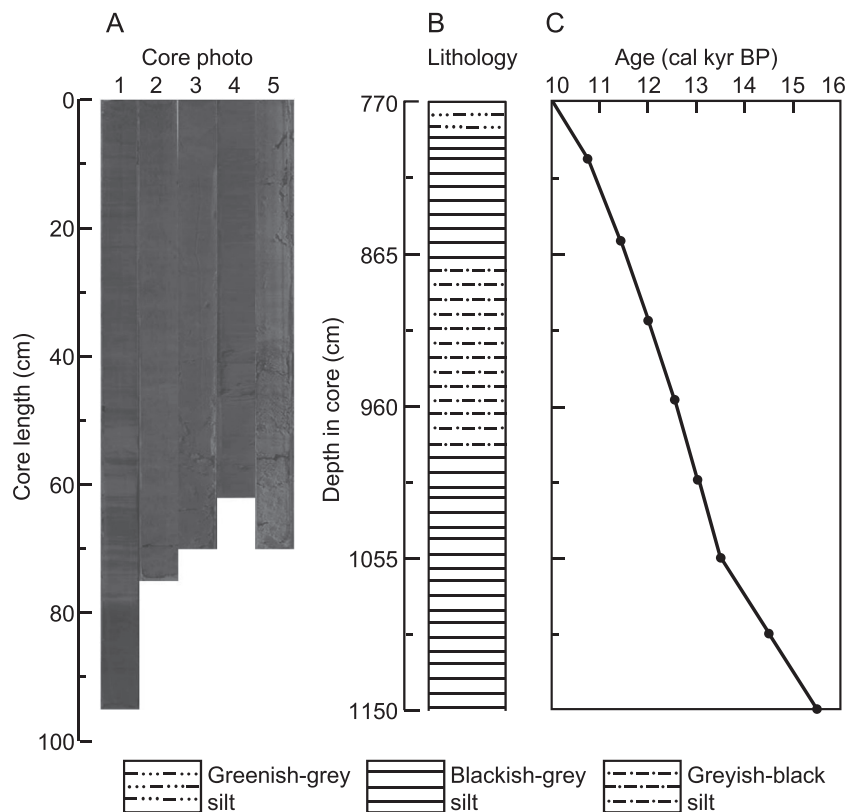


Fig. 3. (A) Photograph of the 7.11–11.83 m of the DL04 core. The 1st section is the interval 711–806 cm, and the 5th section is the interval 1113–1183 cm. (B) Lithology of the 7.7–11.5 m of the DL04 core. (C) Age–depth model for the 7.7–11.5 m of the DL04 core. Solid circles represent the mean values of 2σ ranges of calibrated ages of reservoir-corrected radiocarbon dates.

III system. Samples are ground to a powder finer than 61 μm and pretreated with 1 M HCl for 24 h to remove carbonates, and then rinsed and dried at 40 °C for 24 h. Each sample of 10–15 mg of dried sediment is fully combusted in the Thermo Flash EA 1112 element analyzer at 960 °C for 1–2 min to generate CO₂ for measurements of ¹³C/¹²C ratios. For measurements of ¹⁵N/¹⁴N ratios, each sample of 15–20 mg of dried sediment is fully combusted at 960 °C for 1–2 min to generate NO_x, and the resulting NO_x is then reduced to N₂ by copper at 680 °C. A blank sample, a reference sample (Glycine) and a duplicate sample are routinely analyzed after every five sample measurements. δ¹³C_{org} and δ¹⁵N are expressed in parts per thousand (‰), relative to VPDB and atmospheric nitrogen, respectively. All of the δ¹³C_{org} and δ¹⁵N values are normalized according to the blank sample and Glycine; the certified δ¹³C_{org} and δ¹⁵N values of Glycine are −33.3‰ and 10.0‰, respectively. The precision is better than 0.1‰ for δ¹³C_{org} and 0.2‰ for δ¹⁵N.

3.5. Numerical analyses

Cluster analysis (CONISS, Grimm, 1987) is used to statistically

Table 1
AMS radiocarbon dates of samples from the 7.7 to 11.5 m of the DL04 core. The original radiocarbon dates are cited from Liu et al. (2016).

Laboratory number ^a	Depth interval (cm)	Dating material	δ ¹³ C (‰)	¹⁴ C age (¹⁴ C yr BP)	Corrected ¹⁴ C age (¹⁴ C yr BP)	Calibrated ¹⁴ C age (2σ) (cal yr BP)
PLD-12470	799–798	Organic matter	−31.56	9969 ± 32	9497 ± 39	10,869–10,654
PLD-12472	849–848	Organic matter	−30.84	10,464 ± 37	9992 ± 44	11,640–11,267
PLD-12474	899–898	Organic matter	−27.92	10,715 ± 34	10,243 ± 41	12,141–11,805
PLD-12477	950–949	Organic matter	−31.40	11,050 ± 35	10,578 ± 42	12,670–12,515
PLD-12478	999–998	Organic matter	−31.97	11,630 ± 38	11,158 ± 44	13,117–12,898
PLD-12480	1049–1048	Organic matter	−30.63	12,158 ± 37	11,686 ± 44	13,585–13,431
PLD-12483	1100–1099	Organic matter	−27.39	12,876 ± 42	12,404 ± 48	14,818–14,164
PLD-13857	1150–1149	Organic matter	−27.78	13,436 ± 39	12,964 ± 45	15,713–15,290

^a PLD: Paleo Labo Dating, laboratory code of Paleo Labo Co., Ltd., Japan.

Table 2
Coefficients of determination and P values for the linear correlations between the organic carbon and nitrogen proxies for each stage of the DL04 core from 15,000 to 10,000 cal yr BP. See Fig. 5 for plots of the organic carbon and nitrogen proxies.

Stage	No. of samples	TN vs. TOC	δ ¹³ C _{org} vs. C/N	δ ¹⁵ N vs. δ ¹³ C _{org}
1	26	0.77, positive, P < 0.01	0	0.03, positive, P > 0.05
2	20	0.14, positive, P > 0.05	0	0.03, positive, P > 0.05
3	48	0.70, positive, P < 0.01	0.09, positive, P < 0.05	0.29, positive, P < 0.01

divide the zonation of the time series of TOC and TN concentrations, C/N ratio and δ¹³C_{org} and δ¹⁵N values for the DL04 core from 15,000 to 10,000 cal yr BP. All the raw data of organic geochemical proxies are normalized, and then CONISS is conducted on the normalized data. CONISS is based on the total sum of squares (Grimm, 1987).

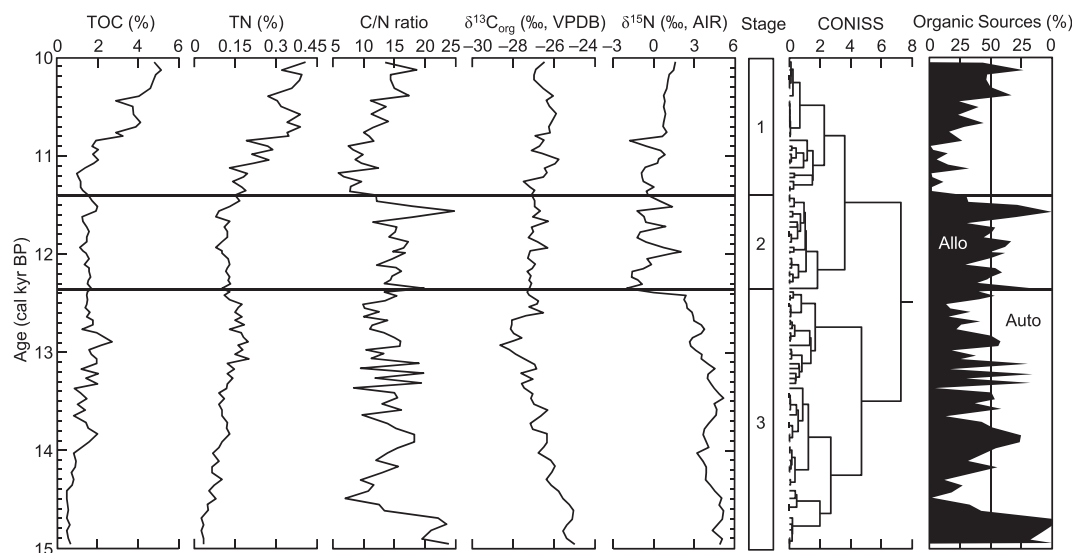


Fig. 4. Time series of total organic carbon (TOC) and total nitrogen (TN) concentrations, atomic TOC/TN (C/N) ratio and organic carbon ($\delta^{13}\text{C}_{\text{org}}$) and nitrogen ($\delta^{15}\text{N}$) isotopic composition for the DL04 core from 15,000 to 10,000 cal yr BP. The original radiocarbon dates are cited from Liu et al. (2016). The radiocarbon data of each sample is derived from the carbon reservoir-corrected age–depth model. Cluster analysis (CONISS) is based on the total sum of squares (Grimm, 1987). Horizontal solid lines indicate the major stages of changes in TOC and TN concentrations, C/N ratio, and $\delta^{13}\text{C}_{\text{org}}$ and $\delta^{15}\text{N}$ values. The organic geochemical data from 11,000 to 10,000 cal yr BP are cited from Fan et al. (2017). The relative proportions of allochthonous (Allo) and autochthonous (Auto) organic matter in the Dali Lake sediments are estimated on the assumption of an average C/N value of 22 for allochthonous organic matter and 8 for autochthonous organic matter, based on the two-end members model (Ishiwatari et al., 2005, 2009; Fan et al., 2017).

4. Results

TOC and TN concentrations, C/N ratio, and $\delta^{13}\text{C}_{\text{org}}$ and $\delta^{15}\text{N}$ values are plotted against calibrated age in Fig. 4. TOC and TN concentrations vary from 0.47% to 5.12% and 0.03% to 0.41%, respectively, yielding a range of 5.89–24.8 for C/N ratio. $\delta^{13}\text{C}_{\text{org}}$ values range from -28.66‰ to -24.99‰ , and $\delta^{15}\text{N}$ values from -1.97‰ to 5.15‰ . The time series of TOC and TN concentrations, C/N ratio, and $\delta^{13}\text{C}_{\text{org}}$ and $\delta^{15}\text{N}$ values from 15,000 to 10,000 cal yr BP can be divided into six stages, e.g., 15,000–14,400, 14,400–13,350, 13,350–12,350, 12,350–11,400, 11,400–10,800 and 10,800–10,000 cal yr BP, based on the stratigraphically constrained cluster analysis (CONISS, Grimm, 1987) (Fig. 4). Considering the similar increasing trends of TOC and TN concentrations and the similar decreasing trends of $\delta^{13}\text{C}_{\text{org}}$ and $\delta^{15}\text{N}$ values from 15,000 to 12,350 cal yr BP, and the generally increasing trends of TOC and TN concentrations, C/N ratio, and $\delta^{13}\text{C}_{\text{org}}$ and $\delta^{15}\text{N}$ values from 11,400 to 10,000 cal yr BP, the data of these five geochemical proxies from 15,000 to 10,000 cal yr BP are divided into three major stages in this study, e.g., 15,000–12,350, 12,350–11,400 and 11,400–10,000 cal yr BP (Fig. 4).

4.1. Stage 3 (1125–930 cm, 15,000–12,350 cal yr BP)

Both TOC and TN concentrations exhibit increasing trends during this stage. TOC concentrations gradually increase from 0.7% to 1.9% from 15,000 to 12,800 cal yr BP with a peak value of 2% at 13,830 cal yr BP, and then decrease to a relatively low level with an average of 1.5% from 12,800 to 12,350 cal yr BP; TN concentrations gradually increase from 0.03% to 0.13% from 15,000 to 12,400 cal yr BP, and then slightly decrease to 0.11% at 12,350 cal yr BP. C/N ratios maintain the highest values with an average of 21.99 from 15,000 to 14,650 cal yr BP, decrease rapidly from 22.13 to 8.87 from 14,650 to 14,400 cal yr BP, and then exhibit an increasing trend and increase from 8.87 to 13.43 from 14,400 to 12,380 cal yr BP with a peak value of 18.26 at 13,910 cal yr BP. Both $\delta^{13}\text{C}_{\text{org}}$ and $\delta^{15}\text{N}$ values display decreasing trends during this stage. $\delta^{13}\text{C}_{\text{org}}$ values gradually decrease from -24.99‰ to -27.31‰ from 15,000 to 12,350 cal yr BP with a trough value of -28.66‰ at 12,930 cal yr BP; $\delta^{15}\text{N}$ values gradually decrease from 4.85‰ to 2.4‰ from 15,000 to 12,420 cal yr BP with two trough

values of 3.21‰ and 2.76‰ at 14,030 and 12,930 cal yr BP, respectively, and then decrease abruptly to 0.04‰ at 12,350 cal yr BP.

4.2. Stage 2 (930–845 cm, 12,350–11,400 cal yr BP)

During this stage, TOC and TN concentrations maintain low levels of averages of 1.5% and 0.12%, respectively. C/N ratios increase to a high level of an average of 15.72 with two peak values of 19.88 at 12,350 cal yr BP and 24.8 at 11,560 cal yr BP. $\delta^{13}\text{C}_{\text{org}}$ values maintain an average of -27.01‰ . $\delta^{15}\text{N}$ values maintain a low level and gradually increase from 0.04‰ to 0.46‰ with a peak value of 2.01‰ at 11,970 cal yr BP.

4.3. Stage 1 (845–770 cm, 11,400–10,000 cal yr BP)

TOC and TN concentrations, C/N ratios and $\delta^{13}\text{C}_{\text{org}}$ and $\delta^{15}\text{N}$ values all display increasing trends during this stage. TOC and TN concentrations increase from 1.5% and 0.15% to 4.7% and 0.41%, respectively. C/N ratios exhibit much lower values than the preceding stage, but increase from 9.9 to 13.5 with fluctuations during this stage. $\delta^{13}\text{C}_{\text{org}}$ values gradually increase from -27.1‰ to -26.47‰ with a peak value of -25.78‰ at 11,040 cal yr BP. $\delta^{15}\text{N}$ values slightly increase from 0.46‰ to 1.61‰ with a trough value of -1.74‰ at 10,840 cal yr BP.

5. Discussion

5.1. Paleoenvironmental implications of the organic carbon and nitrogen proxies

5.1.1. TOC and TN concentrations and C/N ratios

TOC and TN concentrations of the Dali Lake sediments exhibit a good correlation ($R^2 = 0.80$, $P < 0.01$) from 15,000 to 10,000 cal yr BP (Fig. 4), indicating that TN comes mainly from the sedimentary organic matter (Talbot and Johannessen, 1992; Talbot and Lærdal, 2000; Talbot, 2001; Selvaraj et al., 2012). The relatively poorer correlation between TOC and TN concentrations in each stage (Fig. 5; Table 2) may have resulted from various proportions of autochthonous organic matter to the lake sediments (Fig. 4), because TN is mainly

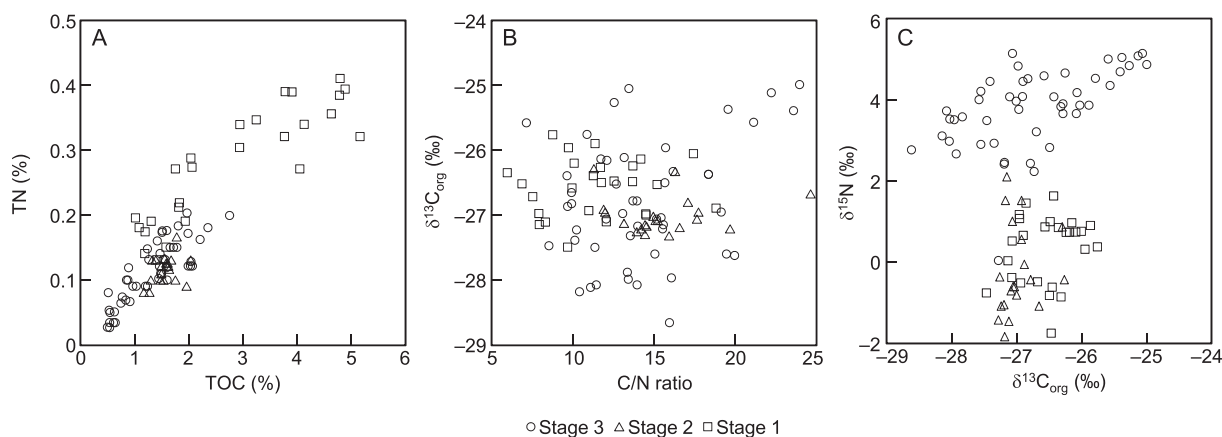


Fig. 5. Biplots of organic carbon and nitrogen proxies for the DL04 core from 15,000 to 10,000 cal yr BP. (A) TN vs. TOC. (B) $\delta^{13}\text{C}_{\text{org}}$ vs. C/N. (C) $\delta^{15}\text{N}$ vs. $\delta^{13}\text{C}_{\text{org}}$. See Table 2 for coefficients of determination and P values for the linear correlations for each stage.

aquatic origin (Meyers, 1990; Talbot and Johannessen, 1992) while TOC represents organic matter from both terrestrial inputs and aquatic production (Meyers, 1994; Lamb et al., 2006; An et al., 2012). Previous studies suggested that organic matter from soils in the Dali Lake catchment could be ignored because it made only a minor contribution to the lake sediments (Fan et al., 2017). In addition, there should be little influence from submerged macrophytes on the sedimentary organic matter in Dali Lake because $\delta^{13}\text{C}_{\text{org}}$ values of the DL04 core from 15,000 to 10,000 cal yr BP (with a maximum of -24.99‰) are much lower than those of submerged macrophytes in alkaline lakes (with an average of -16‰) (Zhang et al., 2004; Aichner et al., 2010, 2012; Qiang et al., 2013). The contribution of emergent macrophytes which might exist in the shallow parts of the lake to the sedimentary organic matter should also be very small, because the water of Dali Lake is alkaline and brackish (Fan et al., 2016) which should be unfavorable for the growth of these macrophytes. Modern observations indicate that aquatic vascular plants are scarce in the Dali Lake and they are generally confined to the areas of the river mouth (Li, 1993; Wang and Dou, 1998). These data provide support for the above inference. However, emergent macrophytes that existed on land near the lake might have contributed, to some extent, to the sedimentary organic matter in Dali Lake. Emergent macrophytes have C/N ratios and $\delta^{13}\text{C}$ values close to those of terrestrial C_3 plants (Meyers and Lallier-Vergès, 1999), therefore the organic matter from emergent macrophytes that grew on land near the lake could be regarded as the allochthonous organic matter (Meyers and Lallier-Vergès, 1999).

Therefore the organic matter in the Dali Lake sediments should come mainly from terrestrial plants and aquatic phytoplankton. C/N ratios can be used to determine the relative contributions of autochthonous and allochthonous organic matter in lake sediments because lacustrine algae are absence of cellulose but rich in protein, therefore organic matter from lacustrine algae commonly have C/N ratios between 4 and 10, while terrestrial organic matter from vascular plants are mainly composed of lignin and cellulose which are nitrogen poor, therefore organic matter from terrestrial plants have relatively high C/N ratios of more than 20 (Meyers, 1990, 1994; Talbot and Johannessen, 1992; Lamb et al., 2006), and degradation and diagenesis of the organic matter have little influence on the trends of changes in C/N ratios (Lamb et al., 2004; Russell et al., 2009). In this study, the two-end members model (Ishiwatari et al., 2005, 2009; Fan et al., 2017) is used and the relative proportions of allochthonous (Allo) and autochthonous (Auto) organic matter in the Dali Lake sediments (Fig. 4) are estimated on the assumption of an average C/N value of 22 for allochthonous organic matter from modern terrestrial plants in the lake catchment and 8 for autochthonous organic matter (Fan et al., 2017). The two-end members model is expressed as follows:

$$\text{C/N}_{\text{mea}} = 22P + 8(1-P)$$

where C/N_{mea} represents the measured atomic C/N values of organic matter from Dali Lake sediments; P and $(1 - P)$ represent the proportions of allochthonous and autochthonous organic matter in the lake sediments, respectively.

It is worth mentioning that the two-end members model is favorable for the identification of the reciprocal relationship between the proportions of allochthonous and autochthonous organic matter in the lake sediments (Fig. 4) and thus for the interpretation of the isotopic data, however, it cannot be used to identify the changes in the absolute amount of allochthonous and autochthonous organic matter because both terrestrial vegetation, terrestrial inputs and aquatic productivity may concurrent increase (Fig. 4) when the regional temperature and precipitation increase (An et al., 2012).

5.1.2. $\delta^{13}\text{C}_{\text{org}}$

The poor correlation between $\delta^{13}\text{C}_{\text{org}}$ values and C/N ratios of organic matter from the Dali Lake sediments (Fig. 5; Table 2) implies that $\delta^{13}\text{C}_{\text{org}}$ values could be influenced by changes in both the relative proportions of terrestrial and aquatic components and the primary isotopic signature of one and/or both. Terrestrial plants are mainly divided into two groups, C_3 and C_4 plants, according to the carbon fixation pathways during the process of photosynthesis (O'Leary, 1988; Farquhar et al., 1989). Almost all trees and cold-season grasses/sedges use the C_3 pathway, and they have an average $\delta^{13}\text{C}$ value of -27‰ ; whereas warm-season grasses/sedges use the C_4 pathway, and they have an average $\delta^{13}\text{C}$ value of -14‰ (O'Leary, 1988; Farquhar et al., 1989). The influence from terrestrial C_4 plants should be excluded because $\delta^{13}\text{C}_{\text{org}}$ values of the DL04 core from 15,000 to 10,000 cal yr BP are much lower than those of terrestrial C_4 plants (Fig. 4).

Aquatic phytoplankton in freshwater lakes has $\delta^{13}\text{C}$ values generally between -32‰ and -26‰ (Meyers, 1994), which are close to those of C_3 plants, while in alkaline lakes phytoplankton have $\delta^{13}\text{C}$ values much higher than those of terrestrial C_3 plants because of their bicarbonate metabolism (Oana and Deevey, 1960; O'Leary, 1988; Farquhar et al., 1989; Zhang et al., 2004; Aichner et al., 2010; Qiang et al., 2013). In the Dali Lake catchment, terrestrial C_3 plants have an average $\delta^{13}\text{C}$ value of -27.1‰ (Wang et al., 2003), which is much lower than those of aquatic phytoplankton due to the alkaline water of the lake (Fan et al., 2016, 2017). Therefore when surface runoffs strengthen due to increases in the regional precipitation, increases in the isotopically lighter, terrestrial organic matter input to the lake would decrease the $\delta^{13}\text{C}_{\text{org}}$ values of sedimentary organic matter. In addition, concurrent increases in the isotopically lighter, riverine dissolved inorganic carbon (DIC) input to the lake would decrease the $\delta^{13}\text{C}$ values of the lake's DIC pool and thus of the aquatic organic matter. While concomitant increases in the nutrients input to the lake

Table 3

An overview of variations in the hydrology and ecology of the Dali Lake basin and changes in the regional temperature and precipitation during the last deglaciation.

Stage	Age interval (cal yr BP)	Terrestrial vegetation and terrestrial inputs	Aquatic phytoplankton	Regional temperature and precipitation
1	11,400–10,000	Both terrestrial vegetation and terrestrial inputs returned to increase	Returned to increase	Both temperature and precipitation returned to increase
2	12,350–11,400	Terrestrial inputs decreased to a relatively low level	Declined to a relatively low status	Temperature decreased significantly at the beginning of this stage, and then maintained a low level; precipitation decreased to a relatively low level
3	15,000–12,350	Both terrestrial vegetation and terrestrial inputs gradually increased	Gradually increased	Both temperature and precipitation gradually increased

may continuously increase the primary productivity of the aquatic phytoplankton, which would in turn increase the $\delta^{13}\text{C}$ values of aquatic organic matter due to progressive enrichment in the ^{13}C of the lake's DIC pool caused by preferential assimilation of $^{12}\text{CO}_2$ by the aquatic phytoplankton (Talbot and Johannessen, 1992; Talbot and Lærdal, 2000).

On the contrary, when regional precipitation decreases significantly, terrestrial C_3 plants may also have relatively high $\delta^{13}\text{C}$ values due to decreases in the isotopic fractionation during the photosynthesis (Wang et al., 2003; Liu et al., 2005). In addition, when large falls in the lake level occur due to significant decreases in the regional precipitation, the limited dissolved CO_2 concentration in the lake water would force aquatic phytoplankton to assimilate more HCO_3^- from the lake water (Calder and Parker, 1973; Pardue et al., 1976; Smith and Walker, 1980; Lucas, 1983), which would produce organic matter significantly enriched in ^{13}C because HCO_3^- has $\delta^{13}\text{C}$ values 7–11‰ higher than dissolved CO_2 (Mook et al., 1974). Nevertheless, it is noteworthy that relatively rapid mixing of lake waters during the period of low lake level would promote the injection of dissolved oxygen into the bottom water. This process could facilitate the degradation of deposited organic matter, leading to releases of isotopically-lighter carbon into the lake water and thus to decreases in the $\delta^{13}\text{C}$ values of aquatic plants and the resulting organic matter (Leng and Marshall, 2004).

5.1.3. $\delta^{15}\text{N}$

$\delta^{15}\text{N}$ values of organic matter in lake sediments can be used to indicate changes in the primary isotopic signature of aquatic organic matter because organic nitrogen in lake sediments is mainly aquatic origin (Meyers, 1990; Talbot and Johannessen, 1992; Fan et al., 2017). The poor correlation between $\delta^{13}\text{C}_{\text{org}}$ and $\delta^{15}\text{N}$ values of organic matter from the Dali Lake sediments (Fig. 5; Table 2) may indicate that the response of the lake's dissolved inorganic nitrogen (DIN) pool to the physicochemical change in the lake water is also very complicated. Lacustrine algae preferentially assimilate ^{14}N from the DIN pool of the lake during the photosynthesis. When primary productivity increases due to increases in the nutrients input to the lake, $\delta^{15}\text{N}$ values of aquatic organic matter will gradually increase due to progressive enrichment in the ^{15}N of the lake's DIN pool (Wada and Hattori, 1978; François et al., 1996). Decreases in $\delta^{15}\text{N}$ values may reflect increases in the input of soil nitrogen into the lake's DIN pool due to increases in the regional precipitation, because soil nitrogen comes initially from atmospheric nitrogen through the fixation of nitrogen-fixing bacteria, atmospherically deposited N and terrestrial plant residues which have $\delta^{15}\text{N}$ values close to 0‰ (Peters et al., 1978; Peterson and Howarth, 1987; Meyers, 1997, 2003; Talbot, 2001), therefore soil nitrogen should have $\delta^{15}\text{N}$ values much lower than those of the lakes' DIN pool (Fan et al., 2017). On the contrary, when lake level significantly falls due to large decreases in the regional precipitation, the lake's DIN pool may be significantly enriched in ^{15}N , as both nitrification in aerobic environments (Talbot and Johannessen, 1992; Talbot and Lærdal, 2000) and ammonia volatilization in alkaline waters (Collister and Hayes, 1991; Talbot and Johannessen, 1992) may occur, and result in significantly high $\delta^{15}\text{N}$ values of the aquatic organic

matter (as high as 18‰). In addition, cold environment ($< 4^\circ\text{C}$) could limit the activities of both nitrifying bacteria (Schindlbacher et al., 2004; Horváth et al., 2010) and ammonifying bacteria (Cloete and Kritzinger, 1985), which would result in sharp decreases in the $\delta^{15}\text{N}$ values of sedimentary organic matter (Sun et al., 2016). Denitrification should have insignificant influence on the $\delta^{15}\text{N}$ value of the lake's DIN pool during the last deglaciation because Dali Lake has a maximum depth of only 11 m at present (Talbot, 2001).

It is also noteworthy that possible limitation of nitrogen in the lake's DIN pool due to high phytoplankton productivity may force blue-green algae to dominate the phytoplankton owing to their capacity of fixing atmospheric nitrogen (Hecky and Kling, 1981, 1987). Shifts in the nitrogen metabolism of the dominant phytoplankton in the lake will cause a sharp decrease in the $\delta^{15}\text{N}$ values of the organic matter (Arthur et al., 1983).

5.2. Environment and climate changes in the Dali Lake region during the last deglaciation

The time series of TOC and TN concentrations, C/N ratio, and $\delta^{13}\text{C}_{\text{org}}$ and $\delta^{15}\text{N}$ values of sedimentary organic matter from the DL04 core can potentially be used to reconstruct the history of variations in the hydrology (surface runoff/fluviol erosion and the lake level) and ecology (terrestrial vegetation development and aquatic phytoplankton productivity) of the lake basin and thus of the climate change in the region during the last deglaciation (Fig. 4; Table 3).

From 15,000 to 12,350 cal yr BP, both TOC and TN concentrations exhibit increasing trends, suggesting that terrestrial vegetation and terrestrial organic matter input displayed increasing trends, and terrestrial nutrient input gradually increased which resulted in continuous increases in the phytoplankton productivity (Håkanson and Jansson, 1983; Talbot and Lærdal, 2000; Cohen, 2003). The interruptions of increases in the TOC concentrations from 12,800 to 12,350 cal yr BP may be related to weaker fluvial erosion due to the development of terrestrial vegetation during the preceding period (Fig. 4). These data imply that regional temperature and precipitation may exhibit increasing trends during this period (An et al., 2012). C/N ratios maintain the highest values with an average close to 22 from 15,000 to 14,650 cal yr BP, denoting that there was little contribution of aquatic organic matter to the lake sediments during this period (Fig. 4). Therefore the highest $\delta^{13}\text{C}_{\text{org}}$ values from 15,000 to 14,650 cal yr BP may indicate that terrestrial C_3 plants had high $\delta^{13}\text{C}_{\text{org}}$ values that may be related to dry climate in the region (Wang et al., 2003; Liu et al., 2005). C/N ratios decrease rapidly from 22.13 to 8.87 from 14,650 to 14,400 cal yr BP, indicating that aquatic organic matter quickly replaced the terrestrial organic matter to dominate the sedimentary organic matter (Fig. 4). Subsequently C/N ratios display an increasing trend with an average of 13.52 from 14,400 to 12,350 cal yr BP, which imply a superimposed influence of both terrestrial inputs and aquatic production on the isotopic characteristics of the sedimentary organic matter in the Dali Lake. Therefore the decreasing trend of $\delta^{13}\text{C}_{\text{org}}$ values from 14,650 to 12,350 cal yr BP may be related to the ^{12}C enrichment of the lake's DIC pool and thus the decreases in $\delta^{13}\text{C}$ values of aquatic organic

matter as a result of large inputs of isotopically-lighter, riverine DIC to the lake (Talbot and Johannessen, 1992; Talbot and Lærdal, 2000). The decreases in $\delta^{13}\text{C}_{\text{org}}$ values may also reflect the contribution of isotopically-lighter, terrestrial organic matter to the lake sediments, due to increases in the regional precipitation (Wang et al., 2003; Liu et al., 2005). The remarkable low $\delta^{13}\text{C}_{\text{org}}$ values correspond to the significantly high TOC concentrations from 13,000 to 12,800 cal yr BP (Fig. 4), supporting the above inference. The positive correlation between $\delta^{13}\text{C}_{\text{org}}$ and $\delta^{15}\text{N}$ values from 15,000 to 12,350 cal yr BP (Fig. 5; Table 2) indicate that the decreasing trend of $\delta^{15}\text{N}$ values may be related to the increases in the isotopically-lighter, soil nitrogen input to the lake that led to the ^{14}N enrichment of the lake's DIN pool (Talbot and Johannessen, 1992; Talbot and Lærdal, 2000), due to increases in the surface runoffs. It is notable that $\delta^{15}\text{N}$ values decrease abruptly to 0.04‰ at 12,350 cal yr BP (Fig. 4). In theory, the lake's DIN pool should be enriched in ^{15}N and the $\delta^{15}\text{N}$ values of the lake's DIN pool should be much higher than 0‰, due to nitrification and/or ammonia volatilization in the lake water (Collister and Hayes, 1991; Talbot and Johannessen, 1992; Talbot and Lærdal, 2000). Therefore it is most likely that water temperature in the Dali Lake largely and rapidly decreased, resulting in limited activities of both nitrifying bacteria (Schindlbacher et al., 2004; Horváth et al., 2010) and ammonifying bacteria (Cloete and Kritzinger, 1985). Significant weakening in the biological activities involving nitrogen cycling in the lake would lead to abrupt decreases in the $\delta^{15}\text{N}$ values of the lake's DIN pool (Talbot and Johannessen, 1992; Talbot and Lærdal, 2000; Sun et al., 2016). The effects of both isotopically-lighter nitrogen input to the lake and nitrogen fixation by blue-green algae on the $\delta^{15}\text{N}$ values of the aquatic organic matter can be excluded because both TOC and TN concentrations do not exhibit such significant changes as $\delta^{15}\text{N}$ values (Fig. 4).

From 12,350 to 11,400 cal yr BP, TOC and TN concentrations maintained a relatively low level, indicating that phytoplankton productivity decreased to a low status which may be resulted from the decreases in the terrestrial inputs or the water temperature or both (Håkanson and Jansson, 1983; Talbot and Lærdal, 2000; Cohen, 2003). C/N ratios increase to a high level of an average of 15.7, suggesting that the proportion of terrestrial organic matter was nearly equal to that of aquatic organic matter (Fig. 4). $\delta^{13}\text{C}_{\text{org}}$ values increase to an average of -27‰ which is slightly higher than the average $\delta^{13}\text{C}$ value of modern terrestrial C_3 plants (-27.1‰) in the lake catchment (Wang et al., 2003). These data imply that regional precipitation may have decreased to a relatively low level during this period, which gave rise to decreases in the isotopic fractionation of terrestrial C_3 plants during the photosynthesis (Wang et al., 2003; Liu et al., 2005), thereby leading to increases in the $\delta^{13}\text{C}$ values of both terrestrial organic matter and riverine DIC, and concurrent increases in the $\delta^{13}\text{C}$ values of the lake's DIC pool and aquatic organic matter. $\delta^{15}\text{N}$ maintain low values of an average of -0.34‰ during this period (Fig. 4), implying that the lake water should be still very cold that limited the activities of nitrifying and ammonifying bacteria (Cloete and Kritzinger, 1985; Schindlbacher et al., 2004; Horváth et al., 2010), which would result in weak nitrification and ammonia volatilization that gave rise to relatively low $\delta^{15}\text{N}$ values of the lake's DIN pool and the organic matter.

From 11,400 to 10,000 cal yr BP, TOC and TN concentrations return to increase, suggesting that terrestrial vegetation returned to develop, terrestrial organic matter and nutrient inputs to the lake increased, and phytoplankton productivity significantly increased, due to increases in the regional temperature and precipitation. C/N ratios exhibit much lower values than the preceding period while increase from 9.9 to 13.5 during this period, indicating that aquatic organic matter dominated the sedimentary organic matter while the proportion of terrestrial organic matter gradually increased (Fig. 4). $\delta^{13}\text{C}_{\text{org}}$ values displayed an increasing trend during this period with maximum values corresponding to the peak values of TN concentrations from 11,100 to 10,900 cal yr BP (Fig. 4). These data indicate that increases in the $\delta^{13}\text{C}_{\text{org}}$ values may be determined by the increases in the phytoplankton productivity.

The progressive ^{13}C enrichment of the lake's DIC pool caused by increased primary productivity overwhelmed the ^{12}C input from terrestrial isotopically-lighter, organic matter and riverine DIC. $\delta^{15}\text{N}$ values maintain a low level of an average of 0.33‰ which is slightly higher than the preceding period (Fig. 4). The relatively low $\delta^{15}\text{N}$ values may indicate an insensitive response of biological activities involving nitrogen cycling in the lake to the regional environment and climate changes or a possible temperature threshold for the recovery of these bacteria (Cloete and Kritzinger, 1985; Schindlbacher et al., 2004; Horváth et al., 2010). Slight increases in the $\delta^{15}\text{N}$ values relative to the preceding period may have resulted from the increases in the phytoplankton productivity (Wada and Hattori, 1978; François et al., 1996; Wu et al., 2007; Xu et al., 2016).

5.3. Possible causes of environment and climate changes in the Dali Lake region during the last deglaciation

The geochemical data of TOC and TN concentrations, C/N ratio, and $\delta^{13}\text{C}_{\text{org}}$ and $\delta^{15}\text{N}$ values of sedimentary organic matter from the DL04 core indicate that regional temperature and precipitation generally exhibited an increasing trend from 15,000 to 12,350 cal yr BP; temperature decreased abruptly at 12,350 cal yr BP and then maintained a low level from 12,350 to 11,400 cal yr BP, precipitation decreased to a relatively low level from 12,350 to 11,400 cal yr BP; and both temperature and precipitation returned to increase from 11,400 to 10,000 cal yr BP (Figs. 4 and 6; Table 3). Recent studies on the environmental magnetism of the DL04 core indicated that pseudo-single domain magnetites were the main magnetic carriers from 15,000 to 12,350 cal yr BP; high concentrations of these relatively coarse magnetic minerals reflected by high values of SIRM and low values of $\chi_{\text{ARM}}/\text{SIRM}$ (Fig. 6) suggest a warm and wet climate during this period (Liu et al., 2016). From 12,350 to 11,400 cal yr BP, the concentrations of magnetic minerals decreased and the magnetic grain size became finer, which was interpreted as less fluvial and runoff transportation due to decreases in the regional precipitation (Liu et al., 2016) (Fig. 6). Increases in the concentrations of magnetic minerals after 11,400 cal yr BP imply an ameliorating regional climate (Liu et al., 2016) (Fig. 6). The regional climate change indicated by the environmental magnetism generally coincides with the geochemical record from sedimentary organic matter of the DL04 core (Fig. 6).

Previous studies on the $\delta^{18}\text{O}$ record of Greenland ice (NGRIP) indicated that several marked temperature fluctuations, such as BA warm phase and YD cold reversal, occurred over northern high latitudes during the last deglaciation (Rasmussen et al., 2006) (Fig. 6). These climate fluctuations have also been reflected in the regional climate change in East Asia. For example, increases in the TOC concentrations and decreases in the $^{13}\text{C}_{\text{org}}$ values of sedimentary organic matter from Moon Lake ($47^{\circ}30' \text{N}$, $120^{\circ}52' \text{E}$) indicated increases in the isotopically lighter, terrestrial organic matter input to the lake, which was related to the increases in regional temperature and precipitation (or effective moisture) in the modern EASM margin during the BA warm period (Liu et al., 2010) (Fig. 1); while decreases in the TOC concentrations and increases in the $^{13}\text{C}_{\text{org}}$ values suggested decreases in regional temperature and precipitation during the YD cold period (Liu et al., 2010). The interpretations of the data of TOC concentrations and $^{13}\text{C}_{\text{org}}$ values in Liu et al. (2010) were supported by the changes in regional humidity reconstructed from pollen assemblages from the same lake published by Wu et al. (2016) (Fig. 6). In addition, the regional precipitation reconstructed from pollen assemblages from Gonghai Lake ($38^{\circ}54' \text{N}$, $112^{\circ}14' \text{E}$) in the modern EASM margin (Chen et al., 2015) and the EASM intensity indicated by the $\delta^{18}\text{O}$ record of stalagmite from Hulu Cave ($32^{\circ}30' \text{N}$, $119^{\circ}10' \text{E}$) (Wang et al., 2001) increased during the BA warm period and decreased during the YD cold period (Figs. 1 and 6). The regional climate change reflected by the geochemical data of sedimentary organic matter from Dali Lake is consistent with these records in the Asian monsoonal region (Wang et al., 2001; Liu et al.,

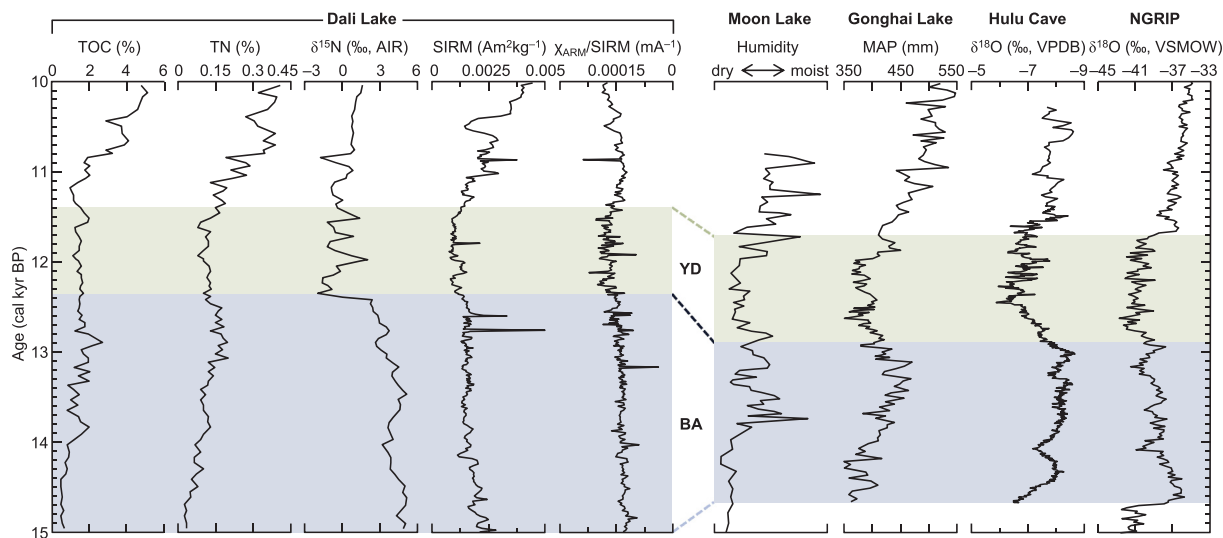


Fig. 6. Correlations of TOC and TN concentrations and $\delta^{15}\text{N}$ values of sedimentary organic matter from the DL04 core from 15,000 to 10,000 cal yr BP with SIRM and $\chi_{\text{ARM}}/\text{SIRM}$ from the same sediment core (Liu et al., 2016); with humidity and mean annual precipitation (MAP) in the modern East Asian summer monsoon margin reconstructed from pollen assemblages of sediment cores from Moon Lake (Wu et al., 2016) and Gonghai Lake (Chen et al., 2015), respectively; and with $\delta^{18}\text{O}$ records of stalagmite from Hulu Cave (Wang et al., 2001) and Greenland ice from NGRIP (Rasmussen et al., 2006), respectively. BA is the abbreviation for Bølling-Allerød and YD is for Younger Dryas.

2010; Chen et al., 2015; Wu et al., 2016) (Figs. 1 and 6) and generally corresponds, within age uncertainties, to the BA warm phase, YD cold reversal and the early Holocene climate amelioration (Fig. 6).

Dali Lake is located in the northern margin of the EASM, and the climate in the region is mainly controlled by the EASM intensity (An, 2000; Xiao et al., 2004). The warm and humid climate in the region is closely related to the strengthening of the EASM (An, 2000). Northern Hemisphere summer insolation (NHSI) changes have been suggested as an important factor forcing variations in the EASM intensity and monsoonal precipitation on orbital timescales (An, 2000). Regional temperature and precipitation reflected by the data of TOC and TN concentrations from Dali Lake as well as regional humidity and mean annual precipitation (MAP) reconstructed from pollen assemblages from Moon Lake (Wu et al., 2016) and Gonghai Lake (Chen et al., 2015), respectively, and EASM intensity indicated by the $\delta^{18}\text{O}$ record of stalagmite from Hulu Cave (Wang et al., 2001) exhibited an increasing trend similar to the gradual increases in the NHSI (Laskar et al., 2004) but different from the gradual decreases in the northern high latitude temperature reflected by the $\delta^{18}\text{O}$ record of Greenland ice (Rasmussen et al., 2006) during the BA warm period (Fig. 6), supporting that the increasing trend of monsoonal precipitation during the BA warm period was driven dominantly by insolation changes. The gradual temperature decrease in the northern high latitudes may have had a relatively limited impact on the monsoonal system, or did not overwhelm the effect of orbital forcing on the strengthening of EASM intensity during the BA warm period. The opposite trends of NHSI and northern high latitude temperature during the BA warm period may explain the relatively smaller magnitude of monsoonal precipitation increase in the Dali Lake region (Fig. 6), or the slight increases in the monsoonal precipitation in East Asia inlands during the BA warm period (Figs. 1 and 6) may reflect a climate threshold (Liu et al., 2014) related to the long distance from source areas of monsoonal moisture to the Asian interior due to relatively lower levels of the East China Seas (Li et al., 2014).

North Atlantic cooling was suggested as a key factor for the weakening in the EASM intensity during the YD cold period, through its influence on the changes in Atlantic Meridional Overturning Circulation (AMOC) and Intertropical Convergence Zone (ITCZ) (Ma et al., 2012). It is plausible that changes in the AMOC and ITCZ would have a great impact on the regional climate in low latitude coastal areas (Wang et al., 2001; Nakagawa et al., 2003; Partin et al., 2015). However, Dali Lake is located in the Asia inlands (Fig. 1), far from

the ITCZ areas. Therefore a mechanism involving atmosphere's dynamic changes was considered to be the linkage between northern high latitude cooling and EASM weakening in the middle latitudes (Fan et al., 2016). It is notable that regional temperature decreased rapidly and significantly recorded by the abrupt decreases in the $\delta^{15}\text{N}$ values of the DL04 core during the transition from BA warm phase to YD cold reversal (Fig. 6). If this temperature signal was true, then the immediate response of temperature in the Dali Lake region to the cooling over northern high latitudes would be identified, which might support the atmosphere's dynamic propagation (Fan et al., 2016). While compared with temperature changes in the northern high latitudes, regional precipitation reflected by the data of TOC and TN concentrations from Dali Lake decreased gradually rather than abruptly at the beginning of the YD cold period and decreased in a much smaller magnitude throughout this period (Fig. 6), which may have resulted from local moisture recycling due to thermal warming at the end of preceding period or from an insensitive response of hydrology and ecology to the regional precipitation change. Persistent moisture transportation from monsoonal source areas to the Asian interior due to NHSI increase should not be considered as a mechanism for the gradual and mild decreases in the regional precipitation during the YD cold period, if frigid airflow indeed prevailed in the Dali Lake region.

Different characteristics and mechanisms regarding regional precipitation changes in East Asia during the YD cold period have been reported recently (Hong et al., 2010; Stebich et al., 2011; Huang et al., 2012; Park et al., 2014; Chen et al., 2015; Yang et al., 2016). For example, the lipid-based paleohydrological record of a sediment core from Dajiuhu peatland indicated an increased precipitation in the middle reaches of the Yangtze River, in response to the regional influence of the western Pacific subtropical high on the residence time of the Meiyu rainband (Huang et al., 2012); the cellulose $\delta^{13}\text{C}$ record of a sediment core from Hani peatland also suggested an increased precipitation in Northeast China, in response to the northward movement of the western Pacific subtropical high (Hong et al., 2010). However, the geochemical records of sedimentary organic matter from Dali Lake and Moon Lake (Liu et al., 2010), the pollen records from Moon Lake (Wu et al., 2016) and Gonghai Lake (Chen et al., 2015), and the stalagmite $\delta^{18}\text{O}$ record from Hulu Cave (Wang et al., 2001) all suggest a decreased precipitation or EASM intensity during the YD cold period, which should be dominantly driven by the northern high latitude cooling (Rasmussen et al., 2006) (Fig. 6).

6. Conclusions

Systematic studies on the characteristic of sedimentary organic matter from Dali Lake provide a detailed record of environment and climate changes in the modern EASM margin during the last deglaciation. Concomitant increases in the TOC and TN concentrations indicate increases in terrestrial organic matter and nutrient inputs to the lake and a development of terrestrial vegetation and phytoplankton productivity, due to increases in the regional temperature and precipitation. C/N ratios reflect changes in the proportions of terrestrial and aquatic organic matter in the Dali Lake sediments. Concurrent decreases in the $\delta^{13}\text{C}_{\text{org}}$ and $\delta^{15}\text{N}$ values generally indicate increases in the isotopically lighter, terrestrial organic matter, riverine DIC and soil nitrogen inputs to the lake, due to increases in surface runoffs; while a sharp decrease in the $\delta^{15}\text{N}$ value implies a significant weakening in the biological activities involving nitrogen cycling in the lake, due to abrupt decrease in the water temperature. The geochemical data indicate that regional temperature and precipitation increased gradually from 15,000 to 12,350 cal yr BP; temperature decreased abruptly at 12,350 cal yr BP and then maintained a low level from 12,350 to 11,400 cal yr BP, precipitation decreased to a relatively low level from 12,350 to 11,400 cal yr BP; and both temperature and precipitation returned to increase after 11,400 cal yr BP. The climate change in the Dali Lake region during the last deglaciation corresponds, within age uncertainties, to the BA warm phase and YD cold reversal in the northern high latitudes. However, the gradual and mild increasing trend of regional temperature and precipitation during the BA warm period contrasts with the general cooling trend in northern high latitude temperature, implying a dominant influence from increases in the NHSI; while the slight decreases in regional precipitation relative to the rapid and significant decreases in northern high latitude temperature during the YD cold period may have resulted from local moisture recycling or from an insensitive response of hydrology and ecology to the regional precipitation change.

Acknowledgements

The authors are grateful to the associate editor Zhonghui Liu and two anonymous reviewers for the improvement of the early version of this manuscript. This study is supported by the National Natural Science Foundation of China (Grant 41672166, 41130101 and 41372188).

References

- Aichner, B., Herzsuh, U., Wilkes, H., 2010. Influence of aquatic macrophytes on the stable carbon isotopic signatures of sedimentary organic matter in lakes on the Tibetan Plateau. *Org. Geochem.* 41, 706–718.
- Aichner, B., Herzsuh, U., Wilkes, H., Hans-Martin, S., Wang, Y.B., Plessen, B., Mischke, S., Diekmann, B., Zhang, C.J., 2012. Ecological development of Lake Donggi Cona, north-eastern Tibetan Plateau, since the late glacial on basis of organic geochemical proxies and non-pollen palynomorphs. *Palaeogeogr. Palaeoclimatol. Palaeoecol.* 313 (314), 140–149.
- An, Z.S., 2000. The history and variability of the East Asian paleomonsoon climate. *Quatern. Sci. Rev.* 19, 171–187.
- An, Z.S., Colman, S.M., Zhou, W.J., Li, X.Q., Brown, E.T., Jull, A.J.T., Cai, Y.J., Huang, Y.S., Lu, X.F., Chang, H., Song, Y.G., Sun, Y.B., Xu, H., Liu, W.G., Jin, Z.D., Liu, X.D., Cheng, P., Liu, Y., Ai, L., Li, X.Z., Liu, X.J., Yan, L.B., Shi, Z.G., Wang, X.L., Wu, F., Qiang, X.K., Dong, J.B., Lu, F.Y., Xu, X.W., 2012. Interplay between the Westerlies and Asian monsoon recorded in Lake Qinghai sediments since 32 ka. *Sci. Rep.* 2, 619. <http://dx.doi.org/10.1038/srep00619>.
- Arthur, M.A., Anderson, T.F., Kaplan, I.R., Veizer, J., Land, L.S., 1983. Stable isotopes in sedimentary geology. *SEPM Short Course* 10, 435.
- Bond, G., Showers, W., Cheseby, M., Lotti, R., Almasi, P., deMenocal, P., Priore, P., Cullen, H., Hajdas, I., Bonani, G., 1997. A pervasive millennial-scale cycle in North Atlantic Holocene and Glacial climates. *Science* 278, 1257–1266.
- Bronk Ramsey, C., Lee, S., 2013. Recent and planned developments of the program OxCal. *Radiocarbon* 55, 720–730.
- Brooks, S.J., Birks, H.J.B., 2001. Chironomid-inferred air temperatures from Lateglacial and Holocene sites in north-west Europe: progress and problems. *Quatern. Sci. Rev.* 20, 1723–1741.
- Calder, J.A., Parker, P.L., 1973. Geochemical implications of induced changes in ^{13}C fractionation by blue-green algae. *Geochim. Cosmochim. Acta* 37, 133–140.
- Chen, F.H., Liu, J.B., Xu, Q.H., Li, Y.C., Chen, J.H., Wei, H.T., Liu, Q.S., Wang, Z.L., Cao, X.Y., Zhang, S.R., 2013. Environmental magnetic studies of sediment cores from Gonghai Lake: implications for monsoon evolution in North China during the late glacial and Holocene. *J. Paleolimnol.* 49, 447–464.
- Chen, F.H., Xu, Q.H., Chen, J.H., Birks, H.J.B., Liu, J.B., Zhang, S.R., Jin, L.Y., An, C.B., Telford, R.J., Cao, X.Y., Wang, Z.L., Zhang, X.J., Selvaraj, K., Lu, H.Y., Li, Y.C., Zheng, Z., Wang, H.P., Zhou, A.F., Dong, G.H., Zhang, J.W., Huang, X.Z., Bloemendal, J., Rao, Z.G., 2015. East Asian summer monsoon precipitation variability since the last deglaciation. *Sci. Rep.* 5, 11186. <http://dx.doi.org/10.1038/srep11186>.
- Cloete, S.W.P., Kritzing, N.M., 1985. A laboratory assessment of various treatment conditions affecting the ammoniation of wheat straw by urea. 1. The effect of temperature, moisture level and treatment period. *S. Afr. J. Anim. Sci.* 14, 55–58.
- Cohen, A.S., 2003. *Paleolimnology: The History and Evolution of Lake Systems*. Oxford University Press, Oxford, pp. 500.
- COHMAP Members, 1988. Climatic changes of the last 18,000 years: observations and model simulations. *Science* 241, 1043–1052.
- Collister, J.W., Hayes, J.M., 1991. A Preliminary Study of the Carbon and Nitrogen Isotope Biogeochemistry of Lacustrine Sedimentary Rocks from the Great River Formation, Wyoming, Utah and Colorado. United States Geological Survey Bulletin 1973-A-G, C1–C16.
- Compilatory Commission of Vegetation of China, 1980. *Vegetation of China*. Science Press, Beijing, pp. 932–955 (in Chinese).
- Dansgaard, W., Johnsen, S.J., Clausen, H.B., Dahl-Jensen, D., Gundestrup, N.S., Hammer, C.U., Hvidberg, C.S., Steffensen, J.P., Sveinbjörnsdóttir, A.E., Jouzel, J., Bond, G., 1993. Evidence for general instability of past climate from a 250-kyr ice core record. *Nature* 364, 218–220.
- Dykoski, C.A., Edwards, R.L., Cheng, H., Yuan, D.X., Cai, Y.J., Zhang, M.L., Lin, Y.S., Qiang, J.M., An, Z.S., Revenaugh, J., 2005. A high-resolution, absolute-dated Holocene and deglacial Asian monsoon record from Dongge Cave, China. *Earth Planet. Sci. Lett.* 233, 71–86.
- Fan, J.W., Xiao, J.L., Wen, R.L., Zhang, S.R., Wang, X., Cui, L.L., Li, H., Xue, D.S., Yamagata, H., 2016. Droughts in the East Asian summer monsoon margin during the last 6 kys: link to the North Atlantic cooling events. *Quatern. Sci. Rev.* 151, 88–99.
- Fan, J.W., Xiao, J.L., Wen, R.L., Zhang, S.R., Wang, X., Cui, L.L., Yamagata, H., 2017. Carbon and nitrogen signatures of sedimentary organic matter from Dali Lake in Inner Mongolia: implications for Holocene hydrological and ecological variations in the East Asian summer monsoon margin. *Quatern. Int.* <http://dx.doi.org/10.1016/j.quaint.2016.09.050>.
- Farquhar, G.D., Ehleringer, J.R., Hubick, K.T., 1989. Carbon isotope discrimination and photosynthesis. *Annu. Rev. Plant Physiol. Plant Mol. Biol.* 40, 503–537.
- Flower, B.P., Hastings, D.W., Hill, H.W., Quinn, T.M., 2004. Phasing of deglacial warming and Laurentide Ice Sheet meltwater in the Gulf of Mexico. *Geology* 32, 597–600.
- François, R., Pilskaln, C.H., Altabet, M.A., 1996. Seasonal variation in the nitrogen isotopic composition of sediment trap materials collected in Lake Malawi. In: Johnson, T.C., Odada, E.O. (Eds.), *The Limnology, Climatology and Paleoclimatology of the East African Lakes*. Gordon and Breach, Amsterdam, pp. 241–250.
- Godwin, H., 1962. Half-life of radiocarbon. *Nature* 195, 984.
- Grimm, E.C., 1987. CONISS: a FORTRAN 77 program for stratigraphically constrained cluster analysis by the method of incremental sum of squares. *Comput. Geosci.* 13, 13–35.
- Grootes, P.M., Stuiver, M., White, J.W.C., Johnsen, S., Jouzel, J., 1993. Comparison of oxygen isotope records from the GISP2 and GRIP Greenland ice cores. *Nature* 366, 552–554.
- Håkanson, L., Jansson, M., 1983. *Principles of Lake Sedimentology*. Springer, Berlin, pp. 316.
- Hecky, R.E., Kling, H.J., 1981. The phytoplankton and protozooplankton of the euphotic zone of Lake Tanganyika: species composition, biomass, chlorophyll content, and spatio-temporal distribution. *Limnol. Oceanogr.* 26, 548–564.
- Hecky, R.E., Kling, H.J., 1987. Phytoplankton ecology of the great lakes in the rift valleys of central Africa. *Ergeb. Limnol.* 25, 197–228.
- Heinrich, H., 1988. Origin and consequences of cyclic ice rafting in the Northeast Atlantic Ocean during the past 130,000 years. *Quatern. Res.* 29, 142–152.
- Herzsuh, U., Zhang, C.J., Mischke, S., Herzsuh, R., Mohammadi, F., Mingram, B., Körschner, H., Riedel, F., 2005. A late Quaternary lake record from the Qilian Mountains (NW China): evolution of the primary production and the water depth reconstructed from macrofossil, pollen, biomarker, and isotope data. *Global Planet. Change* 46, 361–379.
- Hong, B., Hong, Y.T., Lin, Q.H., Shibata, Y., Uchida, M., Zhu, Y.X., Leng, X.T., Wang, Y., Cai, C.C., 2010. Anti-phase oscillation of Asian monsoons during the Younger Dryas period: evidence from peat cellulose $\delta^{13}\text{C}$ of Hani, Northeast China. *Palaeogeogr. Palaeoclimatol. Palaeoecol.* 297, 214–222.
- Horváth, L., Grosz, B., Machon, A., Tuba, Z., Nagy, Z., Czöbel, S.Z., Balogh, J., Péli, E., Fóti, S.Z., Weidinger, T., Pintér, K., Fűrér, E., 2010. Estimation of nitrous oxide emission from Hungarian semi-arid sandy and loess grasslands; effect of soil parameters, grazing, irrigation and use of fertilizer. *Agric. Ecosyst. Environ.* 139, 255–263.
- Huang, X.Y., Meyers, P.A., Yu, J.X., Wang, X.X., Huang, J.H., Jin, F., Gu, Y.S., Xie, S.C., 2012. Moisture conditions during the Younger Dryas and the early Holocene in the middle reaches of the Yangtze River, central China. *Holocene* 22, 1473–1479.
- Ishiwatari, R., Negishi, K., Yoshikawa, H., Yamamoto, S., 2009. Glacial–interglacial productivity and environmental changes in Lake Biwa, Japan: a sediment core study of organic carbon, chlorins and biomarkers. *Org. Geochem.* 40, 520–530.
- Ishiwatari, R., Yamamoto, S., Uemura, H., 2005. Lipid and lignin/cutin compounds in Lake Baikal sediments over the last 37 kyr: implications for glacial–interglacial palaeoenvironmental change. *Org. Geochem.* 36, 327–347.
- Lamb, A.L., Leng, M.J., Mohammed, M.U., Lamb, H.F., 2004. Holocene climate and

- vegetation change in the Main Ethiopian Rift Valley, inferred from the composition (C/N and $\delta^{13}\text{C}$) of lacustrine organic matter. *Quatern. Sci. Rev.* 23, 881–891.
- Lamb, A.L., Wilson, G.P., Leng, M.J., 2006. A review of coastal palaeoclimate and relative sea-level reconstructions using $\delta^{13}\text{C}$ and C/N ratios in organic material. *Earth Sci. Rev.* 75, 29–57.
- Laskar, J., Robutel, P., Joutel, F., Gastineau, M., Correia, A.C.M., Levrard, B., 2004. A long term numerical solution for the insolation quantities of the Earth. *Astron. Astrophys.* 428, 261–285.
- Leng, M.J., Marshall, J.D., 2004. Palaeoclimate interpretation of stable isotope data from lake sediment archives. *Quatern. Sci. Rev.* 23, 811–831.
- Li, G.X., Li, P., Liu, Y., Qiao, L.L., Ma, Y.Y., Xu, J.S., Yang, Z.G., 2014. Sedimentary system response to the global sea level change in the East China Seas since the last glacial maximum. *Earth Sci. Rev.* 139, 390–405.
- Li, Z.G., 1993. *Annals of Hexigten Banner*. People's Press of Inner Mongolia, Hohhot, pp. 1144 (in Chinese).
- Liu, D.B., Wang, Y.J., Cheng, H., Edwards, R.L., Kong, X.G., Wang, X.F., Wu, J.Y., Chen, S.T., 2008. A detailed comparison of Asian monsoon intensity and Greenland temperature during the Allerød and Younger Dryas events. *Earth Planet. Sci. Lett.* 272, 691–697.
- Liu, Q., Li, Q., Wang, L., Chu, G.Q., 2010. Stable carbon isotope record of bulk organic matter from a sediment core at Moon Lake in the middle part of the Daxing'an Mountain range, northeast China during the last 21 ka. *Quatern. Sci.* 30, 1069–1077 (in Chinese with English abstract).
- Liu, S.Z., Deng, C.L., Xiao, J.L., Li, J.H., Paterson, G.A., Chang, L., Yi, L., Qin, H.F., Zhu, R.X., 2016. High-resolution environmental records of the last deglaciation from Dali Lake, Inner Mongolia. *Palaeogeogr. Palaeoclimatol. Palaeoecol.* 454, 1–11.
- Liu, W.G., Feng, X.H., Ning, Y.F., Zhang, Q.L., Cao, Y.N., An, Z.S., 2005. $\Delta^{13}\text{C}$ variation of C_3 and C_4 plants across an Asian monsoon rainfall gradient in arid northwestern China. *Glob. Change Biol.* 11, 1094–1100.
- Liu, X.J., Colman, S.M., Brown, E.T., An, Z.S., Zhou, W.J., Jull, A.J.T., Huang, Y.S., Cheng, P., Liu, W.G., Xu, H., 2014. A climate threshold at the eastern edge of the Tibetan plateau. *Geophys. Res. Lett.* 41, 5598–5604.
- Liu, Z., Otto-Bliesner, B.L., He, F., Brady, E.C., Tomas, R., Clark, P.U., Carlson, A.E., Lynch-Stieglitz, J., Curry, W., Brook, E., Erickson, D., Jacob, R., Kutzbach, J., Cheng, J., 2009. Transient simulation of last deglaciation with a new mechanism for Bølling-Allerød warming. *Science* 325, 310–314.
- Lucas, W.J., 1983. Photosynthetic assimilation of exogenous HCO_3^- by aquatic plants. *Annu. Rev. Plant Physiol.* 34, 71–104.
- Ma, Z.B., Cheng, H., Tan, M., Edwards, R.L., Li, H.C., You, C.F., Duan, W.H., Wang, X., Kelly, M.J., 2012. *Quatern. Sci. Rev.* 41, 83–93.
- Meyers, P.A., 1990. Impacts of late Quaternary fluctuations in water level on the accumulation of sedimentary organic matter in Walker Lake, Nevada. *Palaeogeogr. Palaeoclimatol. Palaeoecol.* 78, 229–240.
- Meyers, P.A., 1994. Preservation of elemental and isotopic source identification of sedimentary organic matter. *Chem. Geol.* 114, 289–302.
- Meyers, P.A., 1997. Organic geochemical proxies of paleoceanographic, paleolimnologic, and paleoclimatic processes. *Org. Geochem.* 27, 213–250.
- Meyers, P.A., 2003. Applications of organic geochemistry to paleolimnological reconstructions: a summary of examples from the Laurentian Great Lakes. *Org. Geochem.* 34, 261–289.
- Meyers, P.A., Lallier-Vergès, E., 1999. Lacustrine sedimentary organic matter records of Late Quaternary paleoclimates. *J. Paleolimnol.* 21, 345–372.
- Meyers, P.A., Teranes, J.L., 2001. Sediment organic matter. In: Last, W.M., Smol, J.P. (Eds.), *Tracking Environmental Change Using Lake Sediments. Physical and Geochemical Methods*, vol. 2. Kluwer Academic Publishers, Dordrecht, pp. 239–269.
- Mook, W.G., Bommerson, J.C., Staverman, W.H., 1974. Carbon isotope fractionation between dissolved bicarbonate and gaseous carbon dioxide. *Earth Planet. Sci. Lett.* 22, 169–176.
- Nakagawa, T., Kitagawa, H., Yasuda, Y., Tarasov, P.E., Nishida, K., Gotanda, K., Sawai, Y., Yangtze River Civilization Program Members, 2003. Asynchronous climate changes in the North Atlantic and Japan during the last termination. *Science* 299, 688–691.
- Nakamura, T., Niu, E., Oda, H., Ikeda, A., Minami, M., Takahashi, H., Adachi, M., Pals, L., Gottang, A., Suya, N., 2000. The HVEE Tandetron AMS system at Nagoya University. *Nucl. Instrum. Methods Phys. Res. B* 172, 52–57.
- North Greenland Ice Core Project members, 2004. High-resolution record of Northern Hemisphere climate extending into the Last Interglacial period. *Nature* 431, 147–151.
- Oana, S., Deevey, E.S., 1960. Carbon 13 in lake waters, and its possible bearing on paleolimnology. *Am. J. Sci.* 258, 253–272.
- O'Leary, M.H., 1988. Carbon isotopes in photosynthesis. *Bioscience* 38, 328–336.
- Pardue, J.W., Scalan, R.S., Van Baalen, C., Parker, P.L., 1976. Maximum carbon isotope fractionation in photosynthesis by blue-green algae and a green alga. *Geochim. Cosmochim. Acta* 40, 309–312.
- Park, J., Lim, H.S., Lim, J., Park, Y.-H., 2014. High-resolution multi-proxy evidence for millennial- and centennial-scale climate oscillations during the last deglaciation in Jeju Island, South Korea. *Quatern. Sci. Rev.* 105, 112–125.
- Parplius, J., Lücke, A., Vos, H., Mingram, J., Srebich, M., Radtke, U., Han, J., Schleser, G.H., 2008. Late glacial environment and climate development in northeastern China derived from geochemical and isotopic investigations of the varved sediment record from Lake Sihailongwan (Jilin Province). *J. Paleolimnol.* 40, 471–487.
- Partin, J.W., Quinn, T.M., Shen, C.-C., Okumura, Y., Cardenas, M.B., Siringan, F.P., Banner, J.L., Lin, K., Hu, H.-M., Taylor, F.W., 2015. *Nat. Commun.* 6, 8061. <http://dx.doi.org/10.1038/ncomms9061>.
- Peters, K.E., Sweeney, R.E., Kaplan, I.R., 1978. Correlation of carbon and nitrogen stable isotope ratios in sedimentary organic matter. *Limnol. Oceanogr.* 23, 598–604.
- Peterson, B.J., Howarth, R.W., 1987. Sulfur, carbon, and nitrogen isotopes used to trace organic flow in the salt-marsh estuaries of Sapelo Island, Georgia. *Limnol. Oceanogr.* 32, 1195–1213.
- Qiang, M.R., Song, L., Chen, F.H., Li, M.Z., Liu, X.X., Wang, Q., 2013. A 16-ka lake-level record inferred from macrofossils in a sediment core from Genggahai Lake, northeastern Qinghai-Tibetan Plateau (China). *J. Paleolimnol.* 49, 575–590.
- Rasmussen, S.O., Andersen, K.K., Svensson, A.M., Steffensen, J.P., Vinther, B.M., Clausen, H.B., Siggaard-Andersen, M.-L., Johnsen, S.J., Larsen, L.B., Dahl-Jensen, D., Bigler, M., Röthlisberger, R., Fischer, H., Goto-Azuma, K., Hansson, M.E., Ruth, U., 2006. A new Greenland ice core chronology for the last glacial termination. *J. Geophys. Res.* 111, D06102. <http://dx.doi.org/10.1029/2005JD006079>.
- Reimer, P.J., Bard, E., Bayliss, A., Beck, J.W., Blackwell, P.G., Bronk Ramsey, C., Buck, C.E., Cheng, H., Edwards, R.L., Friedrich, M., Grootes, P.M., Guilderson, T.P., Hafldadson, H., Hajdas, I., Hatté, C., Heaton, T.J., Hoffmann, D.L., Hogg, A.G., Hughen, K.A., Kaiser, K.F., Kromer, B., Manning, S.W., Niu, M., Reimer, R.W., Richards, D.A., Scott, E.M., Southon, J.R., Staff, R.A., Turney, C.S.M., van der Plicht, J., 2013. INTCAL13 and MARINE13 radiocarbon age calibration curves, 0–50,000 years cal BP. *Radiocarbon* 55, 1869–1887.
- Russell, J.M., McCoy, S.J., Verschuren, D., Bessems, I., Huang, Y., 2009. Human impacts, climate change, and aquatic ecosystem response during the past 2000 yr at Lake Wandakara, Uganda. *Quatern. Res.* 72, 315–324.
- Russell, J.M., Vogel, H., Konecky, B.L., Bijaksana, S., Huang, Y.S., Melles, M., Wattrus, N., Costa, K., King, J.W., 2014. Glacial forcing of central Indonesian hydroclimate since 60,000 yr B.P. *Proc. Natl. Acad. Sci.* 111, 5100–5105.
- Schindlbacher, A., Zechmeister-Boltenstern, S., Butterbach-Bahl, K., 2004. Effects of soil moisture and temperature on NO , NO_2 , and N_2O emissions from European forest soils. *J. Geophys. Res.* 109, D17302. <http://dx.doi.org/10.1029/2004JD004590>.
- Selvaraj, K., Wei, K.Y., Liu, K.K., Kao, S.J., 2012. Late Holocene monsoon climate of northeastern Taiwan inferred from elemental (C, N) and isotopic ($\delta^{13}\text{C}$, $\delta^{15}\text{N}$) data in lake sediments. *Quatern. Sci. Rev.* 37, 48–60.
- Shen, J., Liu, X.Q., Wang, S.M., Matsumoto, R., 2005. Palaeoclimatic changes in the Qinghai Lake area during the last 18,000 years. *Quatern. Int.* 136, 131–140.
- Smith, F.A., Walker, N.A., 1980. Photosynthesis by aquatic plants: effects of unstirred layers in relation to assimilation of CO_2 and HCO_3^- and to carbon isotopic discrimination. *New Phytol.* 86, 245–259.
- Stebich, M., Mingram, J., Moschen, R., Thiele, A., Schröder, C., 2011. Comments on “Anti-phase oscillation of Asian monsoons during the Younger Dryas period: evidence from peat cellulose $\delta^{13}\text{C}$ of Hani, Northeast China” by B. Hong, Y.T. Hong, Q.H. Lin, Yasuyuki Shibata, Masao Uchida, Y.X. Zhu, X.T. Leng, Y. Wang and C.C. Cai [Palaeogeography, Palaeoclimatology, Palaeoecology 297 (2010) 214–222]. *Palaeogeogr. Palaeoclimatol. Palaeoecol.* 310, 464–470.
- Stuiver, M., Grootes, P.M., 2000. GISP2 oxygen isotope ratios. *Quatern. Res.* 53, 277–284.
- Sun, W.W., Zhang, E.L., Jones, R.T., Liu, E.F., Shen, J., 2016. Biogeochemical processes and response to climate change recorded in the isotopes of lacustrine organic matter, southeastern Qinghai-Tibetan Plateau, China. *Palaeogeogr. Palaeoclimatol. Palaeoecol.* 453, 93–100.
- Sun, Y.B., Clemens, S.C., Morrill, C., Lin, X.P., Wang, X.L., An, Z.S., 2012. Influence of Atlantic meridional overturning circulation on the East Asian winter monsoon. *Nat. Geosci.* 5, 46–49.
- Talbot, M.R., 2001. Nitrogen isotopes in palaeolimnology. In: Last, W.M., Smol, J.P. (Eds.), *Tracking Environmental Change Using Lake Sediments. Physical and Geochemical Methods*, vol. 2. Kluwer Academic Publishers, Dordrecht, pp. 401–439.
- Talbot, M.R., Johannessen, T., 1992. A high resolution palaeoclimatic record for the last 27,500 years in tropical West Africa from the carbon and nitrogen isotopic composition of lacustrine organic matter. *Earth Planet. Sci. Lett.* 110, 23–37.
- Talbot, M.R., Lærdaal, T., 2000. The Late Pleistocene-Holocene palaeolimnology of Lake Victoria, East Africa, based upon elemental and isotopic analyses of sedimentary organic matter. *J. Paleolimnol.* 23, 141–164.
- Wada, E., Hattori, A., 1978. Nitrogen isotope effects in the assimilation of inorganic nitrogenous compounds by marine diatoms. *Geomicrobiol. J.* 1, 85–101.
- Wang, G.A., Han, J.M., Liu, T.S., 2003. The carbon isotope composition of C_3 herbaceous plants in loess area of northern China. *Sci. China Ser. D – Earth Sci.* 46, 1069–1076.
- Wang, S.M., Dou, H.S., 1998. *Annals of Lakes in China*. Science Press, Beijing, pp. 324–325 (in Chinese).
- Wang, Y.J., Cheng, H., Edwards, R.L., An, Z.S., Wu, J.Y., Shen, C.-C., Dorale, J.A., 2001. A high-resolution absolute-dated late Pleistocene monsoon record from Hulu Cave, China. *Science* 294, 2345–2348.
- Wen, R.L., Xiao, J.L., Chang, Z.G., Zhai, D.Y., Xu, Q.H., Li, Y.C., Itoh, S., Lomtatidze, Z., 2010. Holocene climate changes in the mid-high-latitude-monsoon margin reflected by the pollen record from Hulun Lake, northeastern Inner Mongolia. *Quatern. Res.* 73, 293–303.
- Wu, J., Liu, Q., Wang, L., Chu, G.Q., Liu, J.Q., 2016. Vegetation and climate change during the last deglaciation in the Great Khingan Mountain, Northeastern China. *PLoS ONE* 11 (1), e0146261. <http://dx.doi.org/10.1371/journal.pone.0146261>.
- Wu, J.L., Huang, C.M., Zeng, H.A., Schleser, G.H., Battarbee, R., 2007. Sedimentary evidence for recent eutrophication in the northern basin of Lake Taihu, China: human impacts on a large shallow lake. *J. Paleolimnol.* 38, 13–23.
- Xiao, J.L., Si, B., Zhai, D.Y., Itoh, S., Lomtatidze, Z., 2008. Hydrology of Dali Lake in central-eastern Inner Mongolia and Holocene East Asian monsoon variability. *J. Paleolimnol.* 40, 519–528.
- Xiao, J.L., Xu, Q.H., Nakamura, T., Yang, X.L., Liang, W.D., Inouchi, Y., 2004. Holocene vegetation variation in the Daihai Lake region of north-central China: a direct indication of the Asian monsoon climatic history. *Quatern. Sci. Rev.* 23, 1669–1679.
- Xu, H., Yu, K.K., Lan, J.H., Sheng, E.G., Liu, B., Ye, Y.D., Hong, B., Wu, H.X., Zhou, K.E., Yeager, K.M., 2016. Different responses of sedimentary $\delta^{15}\text{N}$ to climatic changes and anthropogenic impacts in lakes across the Eastern margin of the Tibetan Plateau. *J. Asian Earth Sci.* 123, 111–118.
- Yancheva, G., Nowaczyk, N.R., Mingram, J., Dulski, P., Schettler, G., Negendank, J.F.W.,

- Liu, J.Q., Sigman, D.M., Peterson, L.C., Haug, G.H., 2007. Influence of the intertropical convergence zone on the East Asian monsoon. *Nature* 445, 74–77.
- Yang, Y.P., Zhang, H.C., Chang, F.Q., Meng, H.W., Pan, A.D., Zheng, Z., Xiang, R., 2016. Vegetation and climate history inferred from a Qinghai Crater Lake pollen record from Tengchong, southwestern China. *Palaeogeogr. Palaeoclimatol. Palaeoecol.* 461, 1–11.
- Yu, Z., Eicher, U., 1998. Abrupt climate oscillations during the last deglaciation in central North America. *Science* 282, 2235–2238.
- Yuan, D.X., Cheng, H., Edwards, R.L., Dykoski, C.A., Kelly, M.J., Zhang, M.L., Qing, J.M., Lin, Y.S., Wang, Y.J., Wu, J.Y., Dorale, J.A., An, Z.S., Cai, Y.J., 2004. Timing, duration, and transitions of the last Interglacial Asian Monsoon. *Science* 304, 575–578.
- Zhai, D.Y., Xiao, J.L., Zhou, L., Wen, R.L., Chang, Z.G., Wang, X., Jin, X.D., Pang, Q.Q., Itoh, S., 2011. Holocene East Asian monsoon variation inferred from species assemblage and shell chemistry of the ostracodes from Hulun Lake, Inner Mongolia. *Quatern. Res.* 75, 512–522.
- Zhang, C.J., Chen, F.H., Shang, H.M., Cao, J., 2004. The paleoenvironmental significance of organic carbon isotope in lacustrine sediments in the arid China: an example from Sanjiaocheng paleolake in Minqin. *Quatern. Sci.* 24, 88–94 (in Chinese with English abstract).
- Zhang, J.R., Lai, Z.P., Jia, Y.L., 2012. Luminescence chronology for late Quaternary lake levels of enclosed Huangqihai lake in East Asian monsoon marginal area in northern China. *Quat. Geochronol.* 10, 123–128.
- Zhou, X., Sun, L.G., Chu, Y.X., Xia, Z.H., Zhou, X.Y., Li, X.Z., Chu, Z.D., Liu, X.J., Shao, D., Wang, Y.H., 2016. Catastrophic drought in East Asian monsoon region during Heinrich event 1. *Quatern. Sci. Rev.* 141, 1–8.
- Zhu, L.P., Wu, Y.H., Wang, J.B., Lin, X., Ju, J.T., Xie, M.P., Li, M.H., Mäusbacher, R., Schwab, A., Daut, G., 2008. Environmental changes since 8.4 ka reflected in the lacustrine core sediments from Nam Co, central Tibetan Plateau, China. *Holocene* 18, 831–839.